

Neurotrophic activity of the Antennapedia homeodomain depends on its specific DNA-binding properties

(neurons/cell culture/differentiation/neurite growth)

ISABELLE LE ROUX, ALAIN HENRI JOLIOT, EVELYNE BLOCH-GALLEGO, ALAIN PROCHIANTZ,
AND MICHEL VOLOVITCH

Centre National de la Recherche Scientifique Unité Recherche Associée 1414, Ecole Normale Supérieure, 46 rue d'Ulm, 75230 Paris Cedex 05, France

Communicated by W. J. Gehring, July 12, 1993 (received for review October 20, 1992)

ABSTRACT In previous reports we have demonstrated that the 60-aa peptide corresponding to the homeodomain of the *Drosophila* protein Antennapedia (pAntp) translocates through the membrane of neurons in culture, accumulates in neuronal nuclei, and promotes neurite growth. To analyze the importance of specific pAntp DNA-binding properties in this phenomenon we have constructed three mutant versions of pAntp that differ in their ability to translocate through the membrane and to bind specifically the cognate sequence for homeodomains present in the promoter of *HoxA5*. We demonstrate that removing two hydrophobic residues of the third helix inhibits pAntp internalization and suppresses its neurotrophic activity. We also show that pAntp neurotrophic activity is lost when mutations are introduced in positions preserving its penetration and nuclear accumulation but abolishing its capacity to bind specifically the cognate DNA-binding motif for homeoproteins. Our results strongly suggest that pAntp neurotrophic activity requires both its internalization and its specific binding to homeobox cognate sequences. We propose that homeoproteins might regulate important events in the morphological differentiation of the postmitotic neuron.

Homeoproteins, first identified as the products of developmental genes in *Drosophila*, are strongly expressed in the developing nervous system of vertebrates and invertebrates (for review, see ref. 1). Although their exact function has not been clearly established, recent data indicate that they participate in central nervous system induction and morphogenesis and also in the establishment of specific neuronal circuits. This latter point is best illustrated by studies showing that a mutation in the gene encoding the homeoprotein unc-4 in the nematode modifies the synaptic input of a distinct subset of motoneurons (2, 3).

The exact function of homeoproteins in the ontogenesis of the vertebrate nervous system is now being studied thanks to homologous recombination studies in the mouse (4–7) and to more classical approaches in *Xenopus* and chicken (8–10). All of these studies, together with a careful description of the patterns of expression of the transcripts during development, clearly point toward a role for homeoproteins in the organization of defined central nervous system structures. However, until recently (11–14), the study of the mode of action of these trans-activating factors has been hampered by the difficulty in identifying structural genes controlled by these homeoproteins.

In fact, possible insights into the mode of action of homeoproteins in the developing nervous system can be deduced from the phenotypic analysis, at the single-cell level, of mutations affecting distinct homeogenes. This procedure has been achieved *in toto* by Doe *et al.* (15) who demonstrated

a cell-autonomous modification of cell fates and axonal trajectories in mutants carrying *ftz*.

In our laboratory, a strategy was developed for studying the role of homeoproteins in early postmitotic rat neurons developing *in vitro*. The principle was to introduce large amounts of the homeodomain of Antennapedia into neurons in culture, expecting that this peptide would compete with endogenous homeoproteins and interfere with their binding to cognate sites present within the genome, thus creating different morphological phenotypes.

Indeed, we observed that mechanical introduction of pAntp, a purified 60-aa peptide corresponding to the homeodomain of the *Drosophila* protein Antennapedia, into rat embryonic neurons in culture enhances neurite outgrowth (16, 17). In addition, and to our great surprise, we also observed that pAntp neurotrophic activity remained intact when the peptide was added directly to the culture medium after seeding of the cells and that, in fact, extracellular pAntp translocated through the cell membrane by a non-energy-dependent mechanism and accumulated within neuronal nuclei (16, 17).

These observations, however, did not allow us to conclude that the neurotrophic effect of pAntp was linked to its occupancy of the cognate sequences present in promoter sequences of homeoprotein-regulated genes. Indeed, diverse artifacts could be invoked, most importantly artifacts related to the very basic nature of pAntp (pI = 11.35), such as a "polyornithin-like" substratum-coating effect or the occurrence of nonspecific interactions with cytoplasmic or nuclear proteins.

To investigate these possibilities we generated different pAntp mutants by creating point mutations. Two mutants have a reduced capacity to specifically bind the homeodomain-cognate sequence present in the *HoxA5* (formerly *Hox-1.3*) promoter (Prom-*HoxA5*) but still can cross the membrane and accumulate in neuronal nuclei. A third mutant peptide does not translocate through the membrane and cannot bind Prom-*HoxA5*. Compared with wild-type pAntp, none of these mutants increased neurite growth, thus strongly suggesting that pAntp activity is linked to the ability of the 60-amino acid-long homeodomain to penetrate into the cells and to form stable complexes with promoter sequences recognized by endogenous homeoproteins.

MATERIALS AND METHODS

***In Vitro* Mutagenesis.** The pAH1 recombinant plasmid contains the coding sequence for the 60 amino acids of the Antennapedia homeodomain inserted into the pET-3a expression vector (18). Two different PCR products were obtained between a primer outside the coding sequence (nt

3968–3983 or nt 4765–4743) and a mutagenic primer inside the sequence ataaagatttggttcGCgaatcggcgcatgaa in the sense strand; the two residues in capital letters allowed the Gln⁵⁰ → Ala mutation and introduced a *Nru* I restriction site. The two PCR products were subcloned into the *Eco*RV site of the Bluescript pKSm vector (Stratagene). The mutant homeobox was then reconstructed by using the *Nru* I site and transferred into expression vector pET-3a to give the recombinant plasmid pAH50A.

The pAH48S mutant plasmid arose during this cloning procedure, when an exonucleolytic activity contaminating the *Nru* I enzyme removed 6 nt. The resulting sequence codes for a deletion mutant where residues 48–50 (tryptophan, phenylalanine, and glutamine) were replaced by a single serine.

To produce pAH40P2, we started from an intermediate recombinant plasmid, pAH39S, in which the *Kpn* I–*Bam*HI segment of pAH1 (nt 30–183 in the homeobox sequence) had been modified to introduce convenient restriction sites corresponding to silent mutations, except for a Cys³⁹ → Ser substitution. Plasmid pAH40P2 was obtained by replacing a *Sph* I–*Bgl* II segment of plasmid pAH39S (nt 106–136 in the homeobox sequence) by a synthetic oligonucleotide restoring Cys³⁹ and leading to the replacement of another 2 aa in the turn, Leu⁴⁰ and Thr⁴¹, by two proline residues.

All experiments were done according to current procedures (19). Enzymes were purchased from Boehringer Mannheim, New England Biolabs, or Cetus, and the oligonucleotides were synthesized on a model 381A DNA synthesizer (Applied Biosystems). All mutants were verified by sequence determination (20).

Preparation of Mutant Homeodomains. Synthesis and purification of peptides expressed in *Escherichia coli* strain BL21(DE3)pLysS were done, as described (16). Metabolic labeling was achieved by transferring the cells (0.3 A600) to M9 medium/0.2% glycerol/10% methionine-free MEM (GIBCO/BRL). After 1 hr of culture the cells were induced for 1 hr with isopropyl β-D-thiogalactoside (1 mM), incubated for 15 min with rifampicine (200 μg/ml), and incubated for a further 5 min with [³⁵S]methionine (Amersham, 30 μCi/ml; 1 Ci = 37 GBq). After a 10-min chase with 5 μM unlabeled methionine the proteins were extracted and purified, as described (16).

Peptide analyses by gel electrophoresis and fluoresceination were done, as described (16). Purified AR3C fusion protein containing pAntp and the C terminus of the Rab3A protein was from Franck Perez (Ecole Normale Supérieure, Paris) (21).

DNA-Binding Properties. Purified peptides (100 ng) were incubated at 4°C for 15 min with a ³²P-5'-labeled double-stranded synthetic oligonucleotide (sequence 5'-ccaactcaccattagtcacagac-3') in the presence of 20 mM Tris·HCl, pH 7.6/80 mM KCl/1 mM MgCl₂/2 mM dithiothreitol/10% (vol/vol) glycerol/bovine serum albumin at 100 μg/ml. Complexes were separated in 10% polyacrylamide gels (preelectrophoresed at 100 V for 1 hr) at 150 V in 45 mM Tris borate, pH 8.3/0.1 mM EDTA.

Peptide Translocation Through the Cell Membrane. Rat embryonic neurons were dissociated from the spinal cord or cortex of embryonic day 14–16 embryos (22) and suspended in Dulbecco's phosphate-buffered saline-glucose (2 × 10⁶ cells per ml) containing DNase I (30 μg/ml, Sigma) and various concentrations (see *Results*) of purified nonmodified or fluorescent peptides. After 2 hr at 37°C with occasional gentle mixing, the cells were centrifuged, washed once in culture medium, plated at the density of 5000 cells per cm² on coverslips or plastic culture wells precoated with polyornithine and laminin (22), and cultured for 1 or 2 days before fixation and morphological analysis. Culture conditions, fix-

ation protocols, and morphological analysis have been described (17, 22, 23).

When radioactive peptides were used, the cells incubated in suspension with ³⁵S-labeled peptides (50,000 cpm) were carefully washed, lysed for 15 min on ice in phosphate-buffered saline containing 0.5% Nonidet P-40, 1 mM Ca²⁺/1 mM Mg²⁺, and the following antiproteolytic agents: Pefablock (0.5 mM), α₂-macroglobulin (1 μg/ml), leupeptin (10 μg/ml), and pepstatin (1 μg/ml). The nuclear and postnuclear fractions were separated by centrifugation at 2000 × *g* over a 0.32 M sucrose layer for 10 min at 4°C. After resuspension of the nuclear pellets, the radioactivity in aliquots of the different fractions was determined.

In some experiments, the peptides were fluoresceinated as described (16) or tagged with a biotin residue. This latter protocol was based on the ability of an activated thiol linked to an aminopentanoic acid and a biotin residue to establish a covalent disulfide bridge with the single cysteine present between helices 2 and 3. The activated thiol–aminopentanoic acid–biotin molecule was provided by D. Derossi (Ecole Normale Supérieure, Paris) and G. Chassaing (Université Pierre et Marie Curie, Paris). Fluorescent or biotinylated peptides were added to the cells in suspension (fluorescent peptides) or to cells previously cultured for 2 days (biotinylated peptides). Cellular localization of fluorescent peptides was directly analyzed after fixation (16).

Localization of the biotinylated peptides was estimated either by confocal microscopy after fixation and incubation with fluoresceinated streptavidin (Amersham) or by SDS/15% PAGE of cellular fractions followed by electrotransfer on Immobilon (Millipore) and development with streptavidin-peroxidase and luminol, according to the indications of the manufacturer (Amersham).

RESULTS

Production of Mutant Antennapedia Homeodomains. We designed pAntp mutant peptides with sizes and isoelectric points similar to those of pAntp but likely to be impaired to various degrees in their DNA-binding properties. Three such peptides were obtained (Fig. 1). (i) pAntp50A has a substitution in position 50 of the homeodomain within the third helix. Position 50 was chosen because of its recognized importance in the specificity of interaction between homeodomains of different classes and their cognate binding sites (24). Among different possibilities we selected the Gln⁵⁰ → Ala modification on the basis of the absence of Ala⁵⁰ in any of the classical homeodomain sequences available today and also because the same modification results in the complete loss of recognition for both Bicoid and Antennapedia target sites (25). Concomitantly, a His³⁶ → Tyr substitution was introduced (Fig. 1).

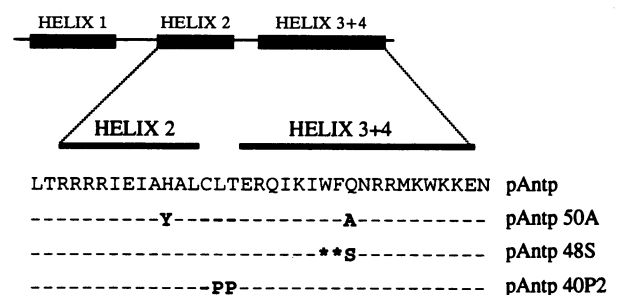


FIG. 1. Structures of mutant Antennapedia homeodomains. Amino acid sequences of the region encompassing helices 2 and 3–4 in the wild-type and mutant homeodomains are in single-letter code; no other differences exist outside this region. ★, Deletions without replacement.

(ii) A second mutant, pAntp48S, corresponds to the replacement of 3 aa (Trp⁴⁸, Phe⁴⁹, and Gln⁵⁰) by a single serine residue (Fig. 1). Trp⁴⁸ and Phe⁴⁹ are conserved in all homeodomains known so far and, therefore, are probably important for homeodomain properties. (iii) A third mutant, pAntp40P2, corresponds to the substitution of Leu⁴⁰ and Thr⁴¹, 2 aa located in the turn between helices 2 and 3, by two proline residues. This modification, which was mimicked by computational imaging (data not shown), impairs correct folding of the helix–turn–helix motif.

DNA-Binding Properties of Wild-Type and Mutant Homeodomains. Fig. 2A shows that wild-type pAntp efficiently retarded Prom-HoxA5, which contains a consensus sequence recognized by many homeoproteins (26). This complex was specific because its formation was inhibited by adding increased amounts of nonradioactive probe. Compared with pAntp, pAntp50A bound poorly to the cognate sequence and was displaced with lower concentrations of unlabeled Prom-HoxA5, suggesting lower complex stability (Fig. 2B). No retardation was visible with pAntp48S or pAntp40P2 (Fig. 2C and D).

To further compare the affinity of pAntp50A with that of pAntp we used a chimeric peptide (called AR3C) encompassing pAntp and the C-terminal region of rab3A, a small GTP-binding protein (21). This chimeric construct—prepared for reasons not related to this study—had a molecular size of 12 kDa. Thus, the retardation bands corresponding to the association of Prom-HoxA5 with pAntp or AR3C could be distinguished by their respective velocities. Fig. 2E and F shows that although pAntp quantitatively displaced the fu-

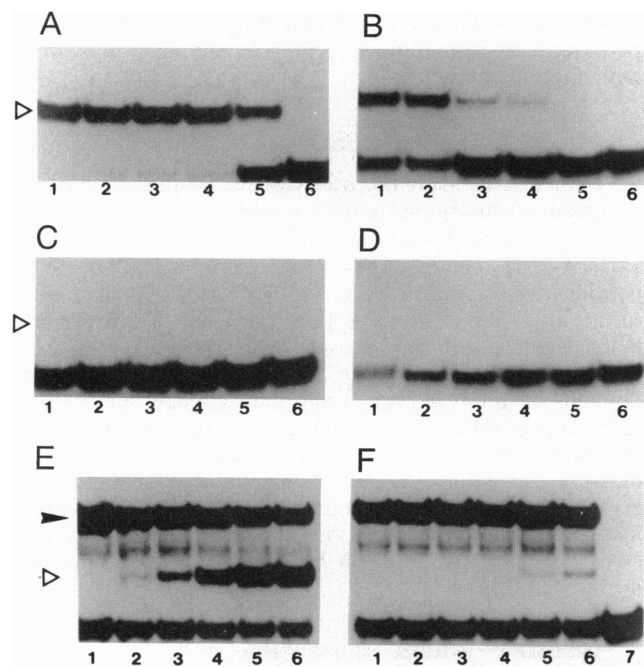


FIG. 2. Specific DNA recognition by wild-type and mutant homeodomains. Prom-HoxA5 target sequence end-labeled with ³²P was incubated with 100 ng of purified pAntp (A), pAntp50A (B), pAntp48S (C), or pAntp40P2 (D), in the presence of various amounts of unlabeled Prom-HoxA5 double-stranded oligonucleotide (none, none, 10, 30, and 150 ng in lanes 1–5, respectively), without (lane 1) or with (lanes 2–5) 10 ng of poly(dI-dC). Lane 6, free probe. Open arrowheads indicate predicted position of complexes. (E and F) Competition in gel retardation of Prom-HoxA5 between 100 ng of AR3C (lanes 1–6) and increased amounts (25, 50, 100, 200, and 300 ng in lanes 2–6, respectively) of either pAntp (E) or pAntp50A (F). Lane 7, free probe alone. Retarded complexes between Prom-HoxA5 and pAntp or pAntp50A are indicated by open arrowheads, and those with the chimeric AR3C peptide are indicated by solid arrowheads.

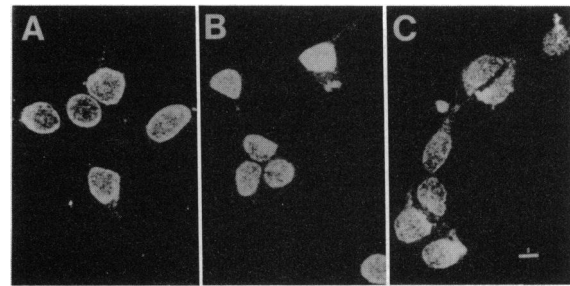


FIG. 3. Distribution of fluoresceinated homeodomains. Embryonic neurons were incubated as described with the following fluoresceinated peptides. (A) pAntp. (B) pAntp50A. (C) pAntp40P2. Visualization is with confocal microscopy. (Scale bar = 5 μ m.)

sion protein at a molar ratio of 2:1, pAntp50A had only a small displacement effect under these conditions.

Peptide Translocation. To analyze translocation and nuclear accumulation of the peptides, they were fluoresceinated and incubated with the dissociated embryonic cells for 2 hr. Cells were then washed, plated, and cultured for 1 day before fixation. Fig. 3 shows by confocal microscopy that pAntp (Fig. 3A), pAntp50A (Fig. 3B), and pAntp40P2 (Fig. 3C) mutants were taken up by all cells in the population, and significant concentrations of the peptides accumulated in the nuclei.

Unfortunately, for nonelucidated structural reasons, possibly because of abnormal folding, pAntp48S could not be fluoresceinated by standard procedures. To study the behavior of this mutant, we developed an original protocol allowing the one-to-one linkage of a biotin residue at the level of the cysteine (Cys³⁹) present between helices 2 and 3 (see *Materials and Methods*). The wild-type pAntp and mutants were

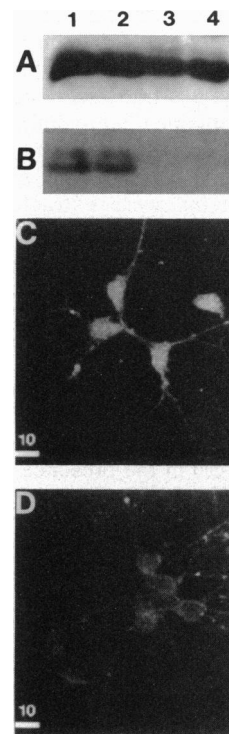


FIG. 4. Internalization of biotinylated peptides. Peptides were modified, as described. (A) Analysis of the four biotinylated peptides by electrophoretic transfer. (B) Only pAntp and pAntp50A peptides are recovered within the cells. Lanes: 1, pAntp; 2, pAntp50A; 3, pAntp40P2; 4, pAntp48S. (C and D) Confocal microscopy sections showing internalization of pAntp (C) and lack of internalization of pAntp48S (D). (Scale bar = 10 μ m.)

Table 1. Measurement of wild-type and mutant homeodomains in different compartments

Homeodomain	Fraction		
	Nuclear, %	Postnuclear, %	Medium, %
pAntp	17.0 ± 6	4.0 ± 1	79.0 ± 6.5
pAntp40P2	11.5 ± 2	1.0 ± 0.5	87.5 ± 2.5
pAntp50A	19.0 ± 5	6.0 ± 1	75.0 ± 6
pAntp48S	2.5 ± 0.5	1.0 ± 0.5	96.5 ± 1

Dissociated rat embryonic neurons treated for 2 hr with purified radioactive peptides were lysed with Nonidet P-40, and the radioactivity in the medium, the nuclear, and the postnuclear fractions was determined. Results are the mean values (±SD) of six different experiments.

labeled in this way, and intensity of the labeling was verified by gel electrophoresis and electrophoretic transfer (Fig. 4A).

Cells were incubated for 1 hr with the modified peptides and washed twice in phosphate buffer, and the proportion of peptide present within the cells was measured by gel electrophoresis and electrophoretic transfer. Fig. 4B shows that modified pAntp and pAntp50A were similarly translocated, whereas the two other biotinylated mutants were not transported through the neuronal membranes. Accordingly, biotinylated pAntp (Fig. 4C) or pAntp50A mutant (data not shown) was seen within the neuronal cells, in contrast with biotinylated mutants pAntp48S (Fig. 4D) or pAntp40P2 (data not shown).

This latter result was, for mutant pAntp40P2, contradictory to that obtained by direct fluorescence. We hypothesize that the addition of a biotin residue linked to Cys³⁹, in direct apposition to the two proline residues, created a structural modification incompatible with transmembrane transport.

This assumption led us to monitor peptide penetration with a third protocol. Peptides labeled in *E. coli* with [³⁵S]methionine were purified and added to dissociated neurons for 2 hr. The medium was then recovered by centrifugation, and after lysis with Nonidet P-40, nuclear and postnuclear fractions were isolated. The radioactive material in the nuclei was analyzed by gel electrophoresis. Autoradiography confirmed that the radioactive species internalized corresponded to the original peptide with no obvious degradation (data not shown).

Peptide distribution was quantified, and the results (Table 1) show that peptides pAntp, pAntp50A, and pAntp40P2 penetrated rapidly and that between 10 and 20% of the peptides reach the nuclei within 2 hr. In fact, pAntp40P2 might be internalized with less efficiency, suggesting that the rigidity created by the two prolines interferes with the internalization process. Strikingly, pAntp48S was the only peptide unable to translocate through the membrane. As previously observed for the wild-type homeodomain and for the chimeric peptides encompassing the homeobox, the penetration of pAntp, pAntp50A, and pAntp40P2 was not reduced by lowering the temperature (data not shown).

In conclusion, it is very likely that all the peptides except pAntp48S translocate through the neuronal membranes and are conveyed to the nuclei.

Neurotrophic Activity. The purified unlabeled peptides were added to dissociated cells for 2 hr. After one wash by centrifugation, cells were resuspended in culture medium, plated at low density, allowing morphological analysis, and cultured for 1 or 2 days before fixation. Fig. 5 illustrates the distribution of rat cortical neurons according to total neurite length and shows that the effect obtained by a 2-hr preincubation with the optimal pAntp concentration of 300 ng per 10⁵ cells (Fig. 5A) was not reproduced with pAntp50A (Fig. 5B),

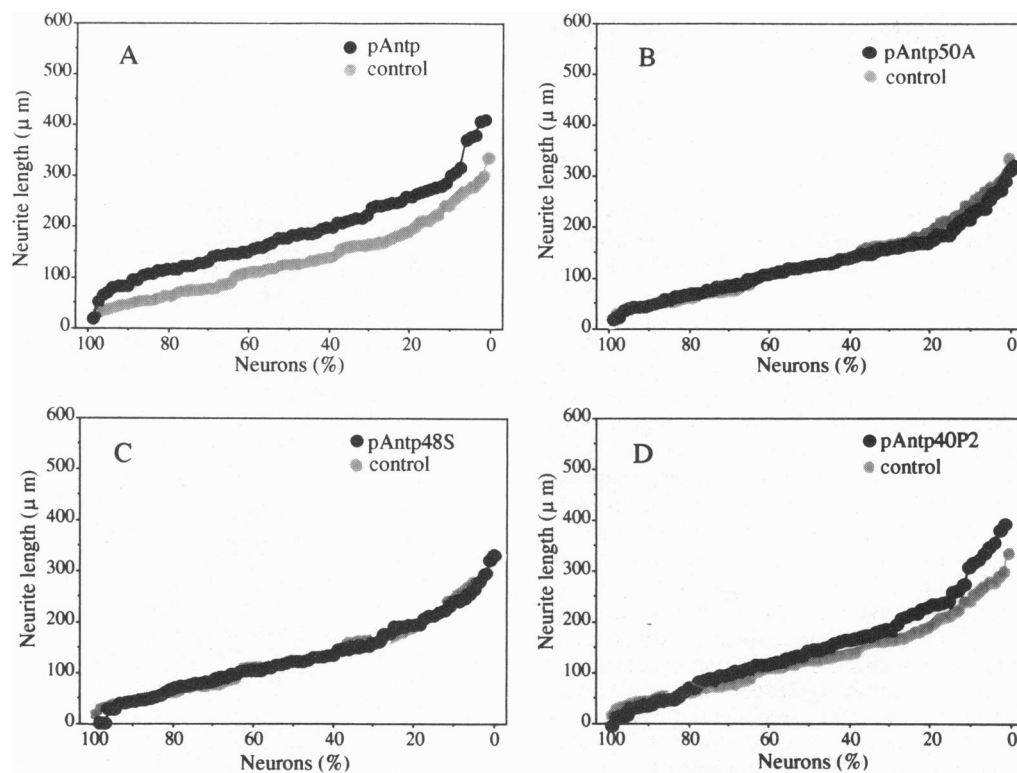


FIG. 5. Cumulative distributions according to total neurite length. This cumulative representation indicates the percentage of neurons with total neurite length higher than the value on the abscissa. For example, in A, the percentage of neurons of neurite length >150 μm increases from 34% (control) to 65% (pAntp). Such distributions can be statistically analyzed (computer program STATWORKS from Cricket Software, Philadelphia). Compared with control, pAntp (A) significantly increased neurite length ($P < 0.001$), whereas mutant homeodomains (B–D) were without effect. Diagrams represent the analysis of 80 neurons for each condition.

pAntp48S (Fig. 5C), or pAntp40P2 (Fig. 5D). A similar absence of stimulation was also seen at higher (up to 900 ng per 10^5 cells) peptide concentrations. The experiment of Fig. 5 is representative of a series of 10 experiments in which we used four different preparations of pAntp and pAntp40P2 and two different preparations of pAntp48S and pAntp50A. In addition, it is noteworthy that identical results were found with different types of neurons and with neurons from different species (23).

DISCUSSION

pAntp mutant derivatives with poor or no DNA-binding capabilities were obtained. pAntp50A (Gln⁵⁰ → Ala) still binds Prom-HoxA5 but does so with a lower affinity than does pAntp. This result is clearly demonstrated in the competition experiments with the unlabeled promoter and the chimeric AR3C peptide. This result corresponds to reports on the importance of position 50 for homeodomain specificity and with the observation that introducing alanine into this position of the Bicoid homeodomain suppresses transactivation (24, 25). The two other mutants cannot specifically bind Prom-HoxA5. For pAntp48S, this effect might be from the Glu⁵⁰ → Ser modification. However, replacing the two hydrophobic residues in positions 48 and 49 could also have influenced pAntp48S-binding properties because these residues appear in all homeodomains sequenced so far. For pAntp40P2, the absence of specific DNA-binding properties is best explained by the modification and rigidity of the turn between helices 2 and 3.

Among the four peptides presented in this study, only one—pAntp48S—was completely unable to translocate through the neuronal membrane. The other peptides, as well as chimeric proteins encompassing the wild-type pAntp, penetrated rapidly at 37°, 12°, and 4°C (data not shown; refs. 17 and 21). It is interesting to note that mutant pAntp48S is lacking two hydrophobic residues partly responsible for the amphiphilic structure of the third helix of pAntp. It is thus plausible that the two hydrophobic residues, Trp⁴⁸ and Phe⁴⁹, participate in a structural motif responsible for pAntp internalization; this would implicate the third helix as the driving force for the internalization of homeobox-containing peptides. Preliminary experiments confirm this hypothesis (D. Derossi, A.H.J., G. Chassaing, and A.P., unpublished work).

The main goal of our present study was to examine whether the reported neurotrophic properties of pAntp (16, 17, 23) were from the specific binding of pAntp to its cognate sequence in the genome or to unspecific phenomena involving the physicochemical properties of the peptide. An obvious artifact is the coating of the substrate by the basic peptide. Indeed, polylysine and other basic polymers are known to increase neurite growth. Our results, which show that three peptides of size and charge similar or identical to those of pAntp do not promote neurite growth, eliminate the possibility that the neurotrophic properties of pAntp reflect a substrate-coating artifact. Another possible pitfall would be that pAntp interacts unspecifically with cytoplasmic or nuclear elements. The lack of neurotrophic properties of pAntp50A and pAntp40P2 also excludes such a possibility.

Our results show that pAntp neurotrophic activity depends on the high affinity and specific DNA-binding properties of the peptides. This result strongly suggests that pAntp acts by interfering with sequences normally recognized by endogenous homeoproteins. In fact, we have verified that the Prom-HoxA5 is recognized by nuclear proteins in cortical neurons and that this interaction can be specifically antagonized by increased concentrations of pAntp (data not shown).

However, the pattern of homeoprotein expression in the developing nervous system is complex, and the diversity of promoters containing homeodomain cognate-binding sequences is high. Thus, elaborating further on a precise mechanism for pAntp neurotrophic activity is difficult. Nevertheless, from our results we can speculate that homeoproteins are involved in the differentiation of postmitotic vertebrate neurons.

We thank Colette Bouillot who helped with the synthesis and purification of homeodomains. This work was supported by Centre National de la Recherche Scientifique, Ecole Normale Supérieure, Université Denis Diderot (Paris VII), and Grants from Ministère de la Recherche et de l'Espace (91.C.0675) and Direction des Recherches et Etudes Techniques (DRET 92-141). A.H.J. and E.B.-G. are fellows from Agence Nationale pour la Recherche sur le SIDA and Association Française contre les Myopathies, respectively.

1. McGinnis, W. & Krumlauf, R. (1992) *Cell* **68**, 283–302.
2. White, J. G., Southgate, E. & Thomson, J. N. (1992) *Nature (London)* **355**, 838–841.
3. Miller, D. M., Shen, M. M., Shamu, C. E., Bürglin, T. R., Ruvkun, G., Dubois, M. L., Ghee, M. & Wilson, L. (1992) *Nature (London)* **355**, 841–845.
4. McMahon, A. P., Joyner, A. L., Bradley, A. & McMahon, J. A. (1992) *Cell* **69**, 581–595.
5. Chisaka, O., Musci, T. S. & Capecchi, M. (1992) *Nature (London)* **355**, 516–520.
6. Le Mouellic, H., Lallemand, Y. & Brulet, P. (1992) *Cell* **69**, 251–264.
7. Lufkin, T., Dierich, L., LeMeur, M., Mark, M. & Chambon, P. (1991) *Cell* **66**, 1105–1119.
8. Cho, K. W. Y., Morita, E. A., Wright, C. V. E. & De Robertis, E. M. (1991) *Cell* **65**, 55–64.
9. Martinez, S., Wassef, M. & Alvarado-Mallard, R. M. (1991) *Neuron* **6**, 971–981.
10. Niehrs, C. & De Robertis, E. M. (1991) *EMBO J.* **10**, 3621–3629.
11. Wagner-Bernholz, J. T., Wilson, C., Gibson, G., Schuh, R. & Gehring, W. J. (1991) *Genes Dev.* **5**, 2467–2480.
12. Jones, F. S., Chalepakis, G., Gruss, P. & Edelman, G. M. (1992) *Proc. Natl. Acad. Sci. USA* **89**, 2091–2095.
13. Jones, F. S., Prediger, E. A., Bittner, D. A., De Robertis, E. M. & Edelman, G. M. (1992) *Proc. Natl. Acad. Sci. USA* **89**, 2086–2090.
14. Violette, S. M., Shashikant, C. S., Salbaum, J. M., Belting, H. G., Wang, J. C. H. & Ruddle, F. H. (1992) *Proc. Natl. Acad. Sci. USA* **89**, 3805–3809.
15. Doe, C. Q., Hiromi, Y., Gehring, W. J. & Goodman, C. S. (1988) *Science* **239**, 170–175.
16. Joliet, A., Pernelle, C., Deagostini-Bazin, H. & Prochiantz, A. (1991) *Proc. Natl. Acad. Sci. USA* **88**, 1864–1868.
17. Joliet, A. H., Triller, A., Volovitch, M., Pernelle, C. & Prochiantz, A. (1991) *New Biol.* **3**, 1121–1134.
18. Rosenberg, A. H., Lade, B. N., Chui, D., Lin, S., Dunn, J. J. & Studier, F. W. (1987) *Gene* **56**, 125–135.
19. Sambrook, J., Fritsch, E. F. & Maniatis, T. (1989) *Molecular Cloning: A Laboratory Manual* (Cold Spring Harbor Lab. Press, Plainview, NY).
20. Chen, E. Y. & Seeberg, P. H. (1985) *DNA* **4**, 165–170.
21. Perez, F., Joliet, A., Bloch-Gallego, E., Zahraoui, A., Triller, A. & Prochiantz, A. (1992) *J. Cell Sci.* **102**, 717–722.
22. Lafont, F., Rouget, M., Triller, A., Prochiantz, A. & Rousset, A. (1992) *Development* **114**, 17–29.
23. Bloch-Gallego, E., Leroux, I., Joliet, A. H., Volovitch, M., Henderson, C. E. & Prochiantz, A. (1993) *J. Cell Biol.* **120**, 485–492.
24. Treisman, J., Gönczy, P., Vashishtha, M., Harris, E. & Desplan, C. (1989) *Cell* **59**, 553–562.
25. Hanes, S. D. & Brent, R. (1989) *Cell* **57**, 1275–1283.
26. Odenwald, W. F., Garbern, J., Arnheiter, H., Tournier-Lasserre, E. & Lazzarini, R. A. (1989) *Genes Dev.* **3**, 158–172.